Sigma J Eng & Nat Sci 38 (2), 2020, 979-993

Sigma Journal of Engineering and Natural Sciences
Sigma Mühendislik ve Fen Bilimleri Dergisi

Research Article

IN-SITU WALL CONCRETE QUALITY USING VELOCITY FIELD-DEPENDENT MIGRATION IN ZIGANA AND TORUL TUNNELS

Işıl SARIÇİÇEK*[1], Aysel ŞEREN[2]

[1]*Ministry of Interior Disaster and Emergency Management Presidency, TRABZON;*
ORCID: 0000-0003-0926-8583
[2]*Karadeniz Technical University, Department of Geophysics, TRABZON;* ORCID: 0000-0003-1134-061X

Received: 24.01.2020 Revised: 06.04.2020 Accepted: 25.05.2020

ABSTRACT

In the scope of this study, the old Zigana and newly-built Torul Tunnels on an important transportation route were selected as the study areas. As the main purpose, monitoring of the distortions in the sidewall concrete lining of the Zigana and Torul tunnels were evaluated by using Diffraction 2D-velocity and Kirchhoff 2D-velocity migrations. Firstly, an artificial radargram was created based on the Finite Difference Time Domain method by taking the model of a tunnel wall structure. Then, for the results obtained from the model, a single velocity value was defined and the migration results were compared. However, as known to all, the outcome of migration by defining a single velocity value from radargrams with too many reflections do not give accurate results. Therefore, the Diffraction 2D-velocity and Kirchhoff 2D-velocity migrations were applied to these radargrams based on the velocity fields and their results were compared. Thus, we suggested that Diffraction 2D-velocity migration gives better results than those of the other in terms of focusing and resolution. When the amplitude slice maps obtained after applying Diffraction 2D-velocity were evaluated, it was observed that deteriorations in the structure continued up to a depth of 75 cm. However, the other type of migration is not very successful to move the distortions to their correct positions after a depth of 37 cm. Thus, in order to apply the migration results correctly, it is recommended to use velocity field.
Keywords: GPR, Zigana and Torul tunnels, 2D velocity field, two migrations types, amplitude-slice maps.

1. INTRODUCTION

The tunnels started to be built in the years 1863 are an important part of highways, waterways, and railways. These tunnels are one of the most important underground structures and widely used for transportation, electric cables, and other purposes. However, the tunnels that are in use have been damaged over time due to structural problems such as fractures and cracks or moisture behind the tunnel coatings [1]. It is very important to investigate these types of problems of the tunnels. For the examining of disorders seen in the tunnels facilitating the transportation of highways; the geological structure of the line where the tunnel is located, the quality of the concrete used during the construction of the tunnel, the fracture-cracked structures found in the concrete, the gaps formed due to water leakage in the concrete are important factors to be considered. During the construction of a tunnel, the ground condition of the tunnel route suffers

* Corresponding Author: e-mail: isil.mataraci61@windowslive.com, tel: (462) 334 12 06 / 1124

from the tunnel structure integrity in the long term and the problems that may arise are grouped into two groups: It is classified a s *(i)* occurring during construction and *(ii)* occurring after opening the building. Concerning the first problem, one of the main reasons for these problems is especially related to the tunnel opened in soft surfaces. Secondly, many factors, such as aging, freezing-thawing, carbonation, and defective construction are among the main causes of ongoing problems as long as a tunnel is used. Depending on these problems, different non-destructive methods (NDT) are used to assess the structural condition of the tunnel [2]. There are ultrasonic tomography (UST) and impulse echo (Impact echo-IE) among the most well-known and used acoustic methods, but Ground Penetrating Radar (GPR) method is one of the most commonly used electromagnetic methods. The GPR method, which can display shallow ground conditions in high resolution, is a successful method of controlling the tunnel units (coating, arch, etc.) and quality. The method is widely used to determine and resolve damages in tunnel improvement studies. Also, this method is a tool practically used in civil engineering works such as pavement analysis [3], bridge and railway monitoring [4], the location of reinforcing bars and metal elements in concrete bases [1], detection of the complex ground problems [5].

The use of GPR method in examining and evaluating important road structures such as bridges and tunnels has emerged as the first evidence of the literature in the 2000s and these studies have increased even more in recent years [1]. Cao et al. (2019) suggested GPR's basic working principle and applied to evaluate the grouting quality. Rathod et al. (2019) discussed the application of GPR and Rebar detector in obtaining valuable information about rebar diameter, spacing and cover depth required to determine the structural capacity of bridge decks. Lin et al. (2020) submitted an alternative way to detect tunnel lining leakage and a reference for the evaluation of structural defects reinforcement in underground engineering.

Therefore, the correct use of GPR in the tunnel structure assessment can help prevent accidents and reduce the risk for human. In this study, two different study areas were examined. The first area, the Zigana tunnel, is an old tunnel that came into use in 1990. The second study area, Torul Tunnel, is a new tunnel that was out of service during data collection. Within the scope of this study, the presence of water-leaking areas and the state of the structure, fracture-crack systems, stratigraphy and deterioration situations of Zigana tunnel walls at 58 km distance from Trabzon on the Trabzon-Gümüşhane highway and also concrete quality of the newly constructed Torul tunnel was aimed to be displayed with GPR method.

2. MATERIAL AND METHODOLOGY

2.1. GPR Method for Tunnel Assessment

GPR transmits electromagnetic energy structure through a transmitting antenna and records the energy reflected through the receiving antenna. Reflections occur at interfaces among materials with different dielectric properties (Figure 1a). The receiving antenna records the time of the received signal and the amplitude of the reflection. This information which is obtained harmlessly with the GPR method indicates the presence and position of voids, discontinuities in concrete.

Depending on technological developments, there are quite different applications with the help of antennas in a very wide frequency range. In tunnel construction which is one of them, GPR sends electromagnetic waves to the tunnel coating at different frequencies. When the transmitted waves encounter a discontinuity in the dielectric properties of the tunnels such as reinforced bars, interface, void, fracture or cracks, some of the waves are reflected and recorded by the receiving antenna. Some parts of the waves can progress deeper into the depths.

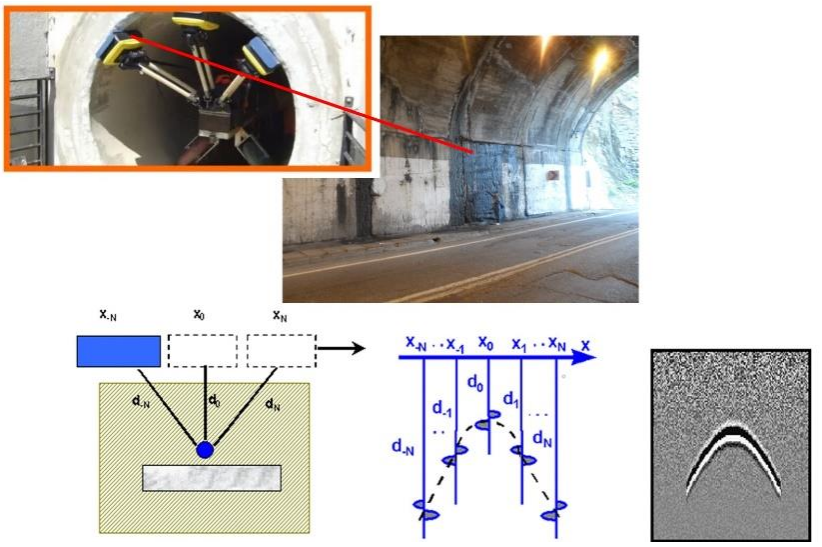

Figure 1. General working principle of radar method [9].

The depth of penetration of radar wave propagating in the environment is related to the conductivity. Penetration depth decreases with increasing conductivity. While the dielectric constant determines the velocity of the propagation of the electromagnetic wave, at the same time, the difference between these dielectric constants is defined as an interface. Also, the dielectric constant determines the area that covered by the electromagnetic wave in the environment. Two-way travel time (t) recorded in GPR method can be expressed as follow:

$$t = \sqrt{4d^2 + x^2}/v \cong 2d/v \tag{1.1}$$

where d; the depth of buried depth of the investigated target, x; the distance between the receiving and transmitting antennas and v; shows the propagation velocity of the electromagnetic wave in the environment. The mean value of the velocity must be known to determine the depth (d) from the interface causing reflection to the measurement plane. The propagation speed of the electromagnetic wave in the environment,

$$v = c/\sqrt{\varepsilon_r . \mu_r} \cong c/\sqrt{\varepsilon_r} \tag{1.2}$$

where $c = 0{,}29979 m/ns$ (the propagation speed of an electromagnetic wave in the cavity), ε_r: the relative permittivity of the medium and μ_r: the relative permeability of the medium (generally$\mu_r = 1$).

If the dielectric constant of the investigated environment is known, velocity information can be obtained from equation (1.2). In cases where this constant is unknown, velocity information is determined with the help of the velocity field based on the reflections arisen from the problems in the structure. In the context of this study, velocity information was obtained by using the velocity field

2.2. Velocity Estimation with Hyperbola Fitting Method

In order to determine the velocity of electromagnetic wave propagation in an environment, different methods have been used [10]. One of the most commonly used among these is the hyperbolic fitting method due to buried reflectors (e.g. fractures) or buried cylindrical shaped objects (e.g. rebar layer, pipes). Among the factors affecting the shapes of these hyperbolas, the

structure of the underground reflector, the relative permeability of the environment in which the objects are located, and the physical conditions of these two substances are of great importance. Therefore, the hyperbolic geometry method (Figure 2), also known as curve fitting is widely applied to estimate the velocity of electromagnetic wave propagation in much software.

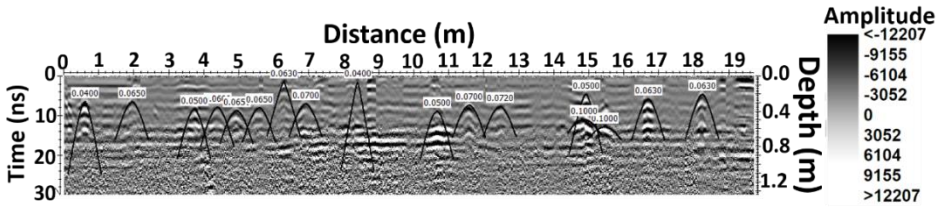

Figure 2. Example of velocity estimation by curve fitting method of data collected Zigana tunnel.

3. STUDY AREA

3.1. Case Study: Zigana Tunnel

Zigana Tunnel is a gateway in the North Anatolian Mountains, within the boundaries of Gümüşhane province. This gateway is located at the transition point between the Eastern Black Sea geographical structure and the central Anatolian plateaus. Due to some difficulties in access to this gate, the tunnel was opened to provide accessibility from the Zigana Mountains on Trabzon-Gümüşhane highway. It is 58 km from Trabzon. Its construction started in 1975 and it came into use in 1990. The length of the tunnel is 1702 m, the height is 8.5 m, and the width is 11.2 m. The altitude is 2032 meters. In some parts of the Zigana tunnel, which is the first working area, the presence of fracture-cracks and water content on the surface was observed (Figures 3,4). Due to the effects of freezing-thawing, carbonation based on intense weather conditions at the Zigana Tunnel and its surroundings, the alteration of problems on the surfaces based on depth is important. In this study area, Kızılkaya formation consisting of clayey limestone, sandy limestone, and tuff intercalated dacite and pyroclastic and Çağlayan formation composed of limestone, sandstone intercalated andesite and basalts are found. The geology of the Zigana tunnel line is defined as Kızılkaya Formation.

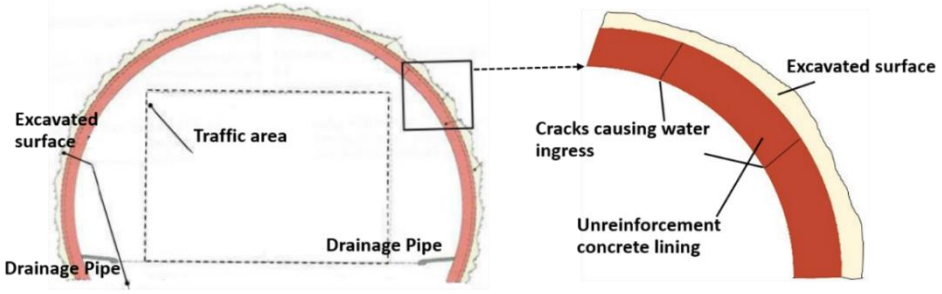

Figure 3. Zigana Tunnel design and pavement structure belonging to tunnel [11].

3.2. Case Study: Torul Tunnel

Another work area on the Trabzon-Gümüşhane highway is the Torul Tunnel (Figure 4c). This tunnel was opened in 2013. The length of the tunnel is 1090 meters and altitude is 1061 meters. Since this tunnel is newly opened, distortion is not observed on the surface. The Çatak formation

carved for the construction of the Torul tunnel is defined by Güven (1993) for the first time and consists of dark gray-green andesite-basalt and pyroclastic. Claystone, sandstone, mudstone, tuffite levels are encountered as intercalations. It is usually in gray-green color. In the northern zone of the Eastern Pontide, tholeiitic and calcalkalen volcanic rocks which were formed in the early period of the Upper Cretaceous spread in a deep marine environment and piled up as volcano-sedimentary rocks. The age of the formation which conformed to the Berdiga formation (Pelin, 1977) is Upper Cretaceous (Turonian-Coniacian-Santonian).

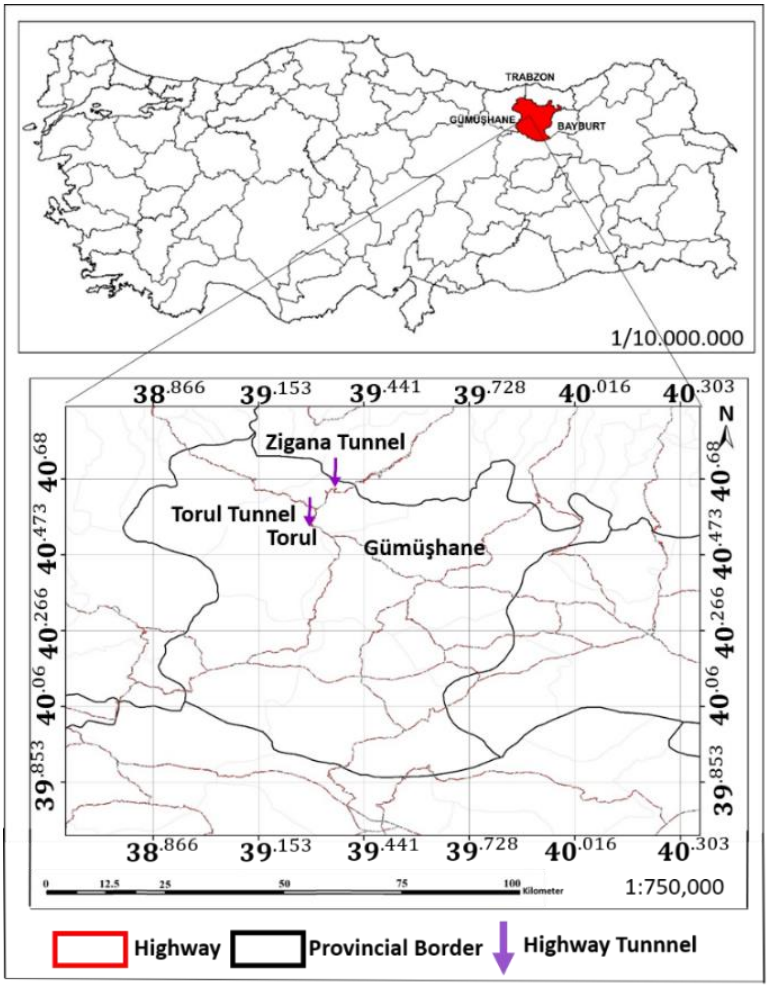

Figure 4. a) Location map of study areas.

4. FDTD SIMULATION

As part of this study, it is aimed to numerically model reinforcements of the Torul tunnel whose structure content has known and to examine the GPR responses. The commonly known finite-difference time-domain method is used for this modeling application. This method, which is

used to model the GPR signal response from complex targets [14], is an explicit and accurate technique. Both the distance and the time steps are discretized and the numerical results are obtained repeatedly in the time domain. The choice of distance and time steps is important, because if they are smaller, the FDTD model defines reality better.

In this study, the effect of known reinforcement bars on radargrams in the structure of the sidewall of the Torul tunnel with a solid concrete structure constitutes the basis of the model. For this purpose, a model with a dimension of 1 m depth and 6 m distance was created (Figure 5a). Thus, for the reinforcing bars found in the concrete-containing structures, the model was formed based on the dielectric constant, conductivity and magnetic permeability values given in the literature [15] (Figure 5a) and the artificial radargram was calculated by using 500 MHz central frequency antenna. The dielectric constant for concrete was taken as $\varepsilon_b = 7$. The dielectric constant of iron was taken as $\varepsilon_d = 1{,}45$. Both the magnetic permeability of the concrete and the magnetic permeability of the iron were taken as $\mu = 1$. Since the concrete is a substance formed by the addition of sand and water, the conductivity of these two substances was taken as $\sigma_b = 0.001$ S/m. The conductivity of the iron was taken as $\sigma_d = 9.93 \times 10^6$ S/m. Besides, the radius of the reinforcement iron was selected to be 8 mm. The artificial radargram was calculated by the help of this model (Figure 5b).

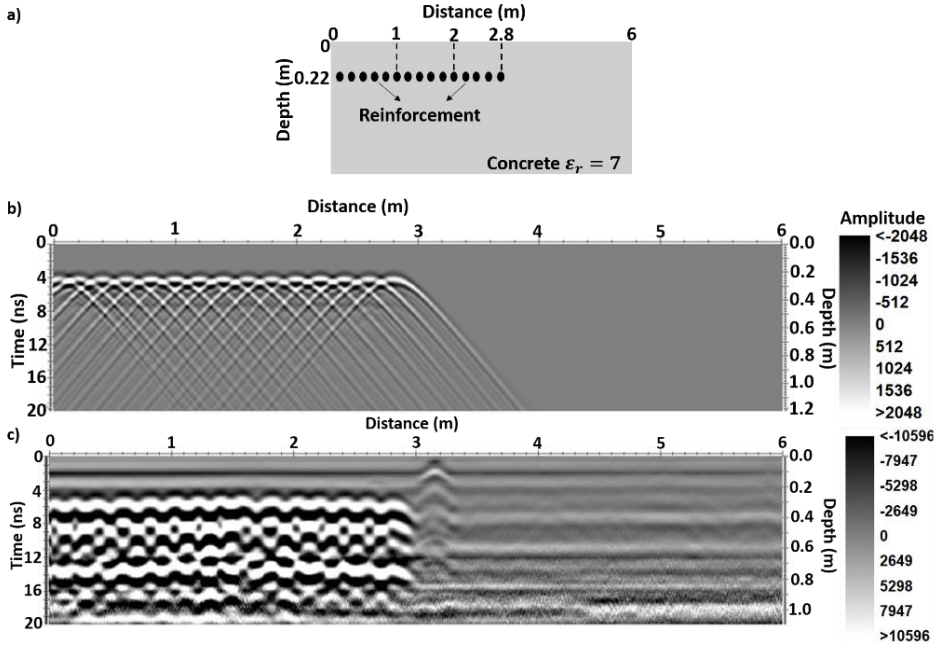

Figure 5. a) FDTD numerical model for Torul tunnel b) Result of numerical model acquired with 500 MHz antenna c) Data of 500MHz GPR acquired from the study area.

When the result of the artificial radargram (Figure 5b) obtained from the numerical model defined in Figure 5a is examined; the iron reinforcements, positioned at equal distances, have shown themselves as small hyperbolic reflections adjacent to each other, such as results obtained from real field data (Figure 5c). Since the created model has one-meter depth and it is observed as small hyperbolic reflections adjacent to each other, reflections from deeper were not taken into account (Figure 5c).

5. DATA ACQUISITION AND DATA PROCESSING

The length of the Zigana Tunnel on the Trabzon-Gümüşhane highway is 1702 m. Throughout the tunnel, it is seen that there are some water leaks at certain distances from both entry openings and therefore, fractures and cracks have been come in sight over time in the coating concrete resulting from these leaks. Also, two different field data were collected with the ground radar method to evaluate the concrete quality. This data was taken using 500 MHz shielded antenna at 30 cm profile intervals in the E-W (east-west) direction. As part of this study, measurements were taken in 10 profiles in the sections where the most intense fractures observed from the surface in the Zigana tunnel (Figures 6a, 6b and 6c).

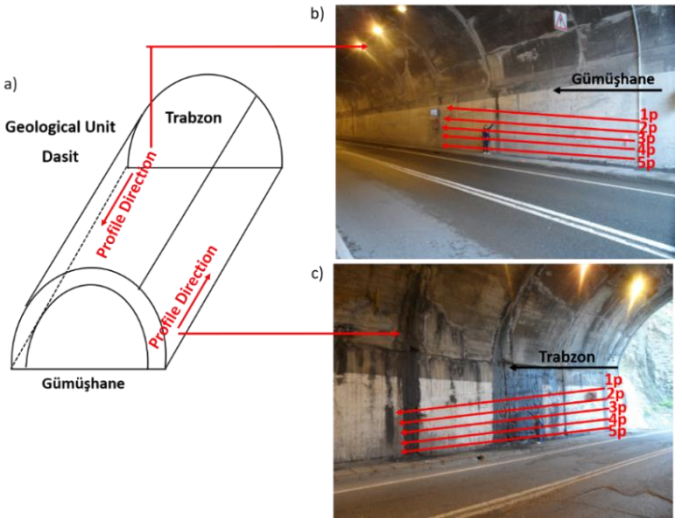

Figure 6. a) Zigana tunnel profile directions b) GPR measurement profiles (Trabzon entry) c) GPR measurement profiles (Gümüşhane entry).

In the Torul tunnel, the other study area, 5 profiles were collected from a single entrance (Figures 7a, 7b and 7c).

Due to the complex nature of the tunnel and the impact of the geological environment, the interpretation of GPR's raw data is complex and there are noisy signals and unwanted noises (multiple reflection waves, traffic intensity, etc.) throughout the research surface. A rich part of water content and the attenuation of the resulting electromagnetic waves also conceal the region where the fracture-cracked type structures are found in the radar image. Therefore, data processing steps must be applied to interpret the raw data. The data processing steps given in Table I have been applied to convert the GPR data obtained from the study areas into better interpretable radargrams.

Table 1. Data processing steps applied to GPR data obtained with 500 MHz shielded antenna

Step	*Data Processing*
1	Subtract-mean (Dewow) (timewindows = 2ns)
2	Gain function (Energy-decay) (scaling value =1)
3	Background removal
4	Move start time
5	Time cut

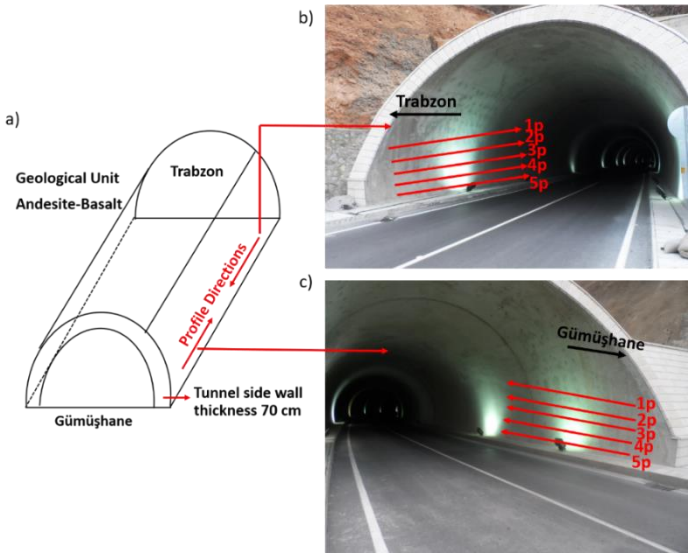

Figure 7. a) Torul tunnel profile directions b) GPR measurement profiles (Trabzon entry) c) GPR measurement profiles (Gümüşhane entry).

To bring the scattered reflections to their correct positions and to obtain a more accurate environment section, it is thought to implement advanced data processing steps. Therefore, the velocity field is determined by the hyperbolic adaptation method, depending on the hyperbolic reflections on the different depth and distances of the GPR sections. As a result, migration techniques were applied to radargrams with the help of this field.

In geophysical measurements, the process of transporting to the point reflecting the reality of a signal which is reflected and recorded from a sloped reflector or a point source within the ground is called migration. Some techniques are used to bring raw GPR images to the correct underground locations. Electromagnetic wave velocities of the investigated structures are usually given in the literature [16]. However, the application of the whole section migration process with a single-velocity value may result in erroneous results. For this reason, in the radar sections where are many scattered hyperbolic reflections at different locations and depths, the 2D velocity field was formed depending on the depth and the migration process was performed with the help of this field. Accordingly, Diffraction 2D-velocity and Kirchhoff 2D-velocity migration techniques were applied and they were tried to investigate how they exhibit results on the same data.

6. RESULTS AND DISCUSSIONS

In this study, an artificial radargram was obtained for sidewall of the Torul tunnel which has a solid concrete structure. There are reinforcing bars which are known their positions. Diffraction 2D-velocity and Kirchhoff 2D-velocity migration were applied to this radargram. In these obtained radargrams, both types of migrations moved the reflectors to their correct positions. However, Diffraction 2D-velocity migration focused the reflectors better than Kirchhoff 2D-velocity migration (Figure 8b).

Field data with the basic data processing steps obtained from the Torul Tunnel, whose environmental characteristics are known, was shown in Figure 9(a). These radargrams (Figure 9b and 9c), which are generated by applying the same migration, confirm the result of the migration on the artificial radargrams.

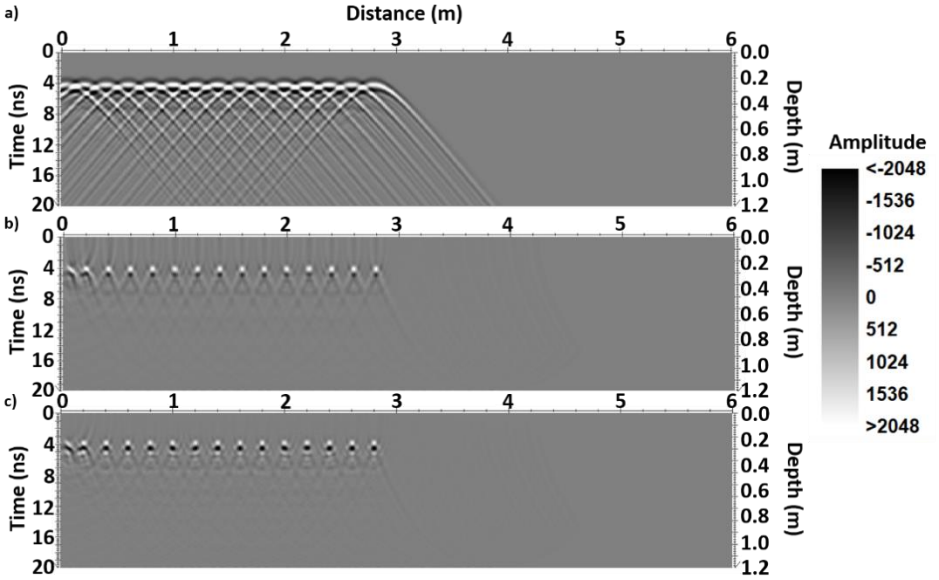

Figure 8. a) Artificial radargram obtained from the model in Figure 5 b) Diffraction 2D-velocity applied and c) Kirchhoff 2D-velocity applied artificial radargram.

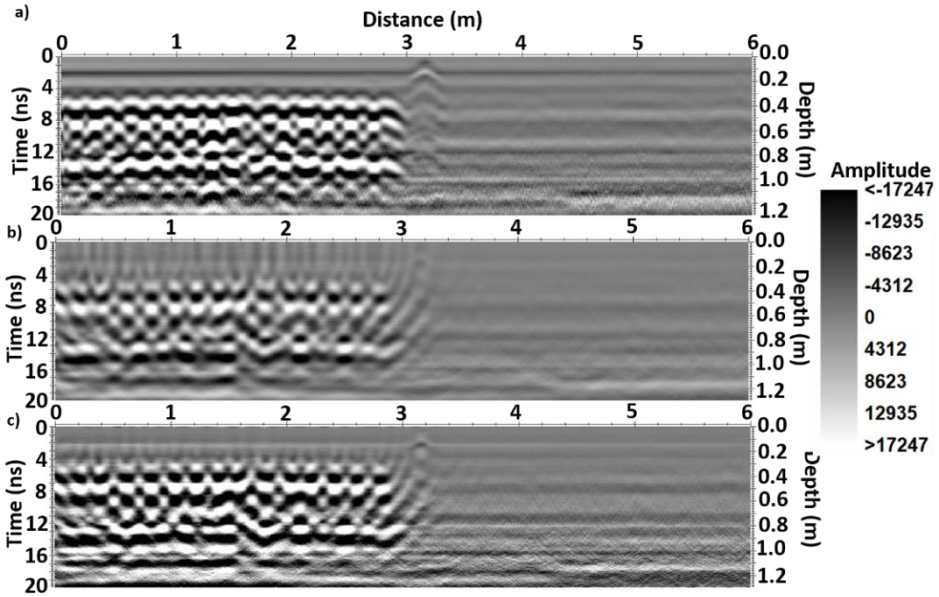

Figure 9. a) The acquired radargram from Torul Tunnel with 500 MHz antenna b) Diffraction 2D-velocity applied and c) Kirchhoff 2D-velocity applied radargram.

In this study, GPR data were collected in the Zigana tunnel and GPR sections were obtained by applying the basic data processing steps shown in Table I (Figure 10). In the Zigana tunnel

which is the first area of study, the most disturbing parts observed from the surface were evaluated. When these radargrams were examined, it was observed that a fracture (red arrows) observed from the surface during measurement of profiles 1-2 continuing for a distance of 2 m and a depth of about 45 cm. The fracture which was observed from the surface at approximately 6 m gave a strong reflection on all profiles. Although fractures were not observed from the surface on the profiles 3-4, these fractures were considered to be in the structure (red arrows). The water leakage on the structure was observed as the attenuation of the electromagnetic wave (red dashed line) in the radargrams of all profiles (Figure 10).

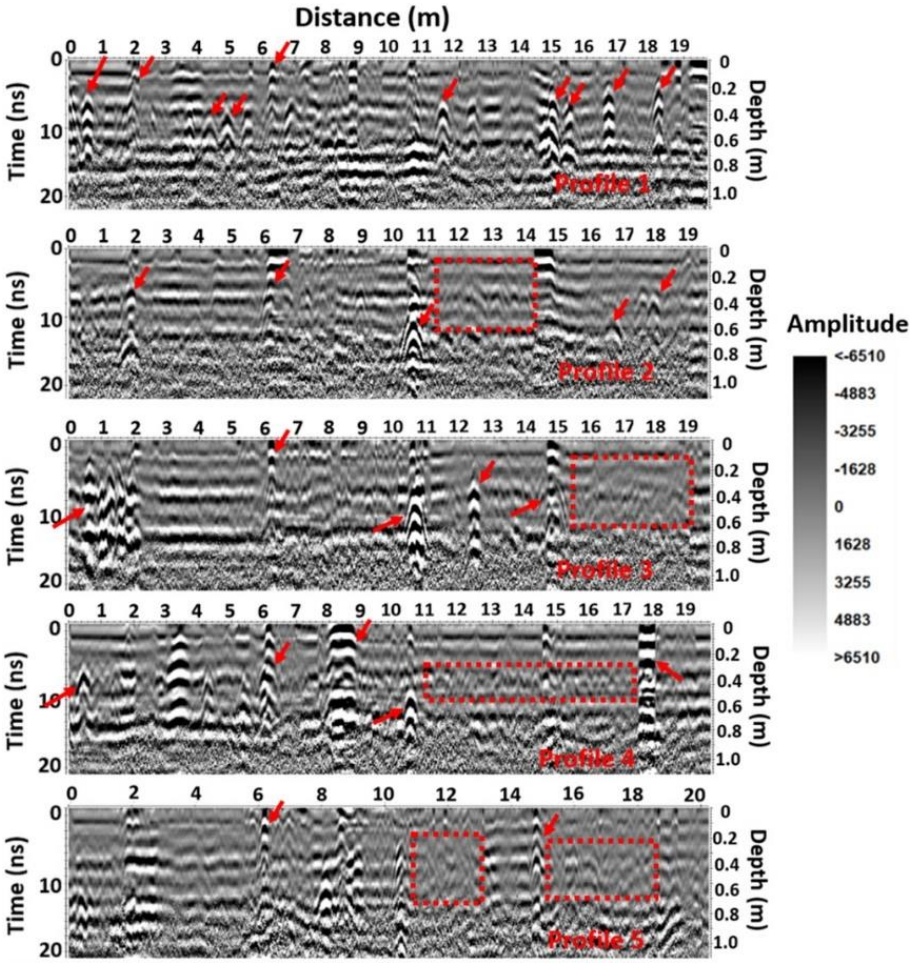

Figure 10. Radargrams of 1-5. profiles obtained with 500 MHz antenna in the Zigana tunnels.

In Figure 10, two types of migration based on the velocity field were applied to enhance images, to bring scattered reflections to their actual locations and to obtain a more accurate media section. The results of these migration types applied to the same radargrams with the help of the speed fields were compared. The radargrams applied to the Diffraction 2D-velocity migration technique are shown in Figure 11. When these radargrams are examined, all fractures (yellow

dashed line) at 2, 6 and 16.5 m distances and different profiles observed from the surface defined in the radargram of Figure 10 were tried to move to their actual positions in Figure 11.

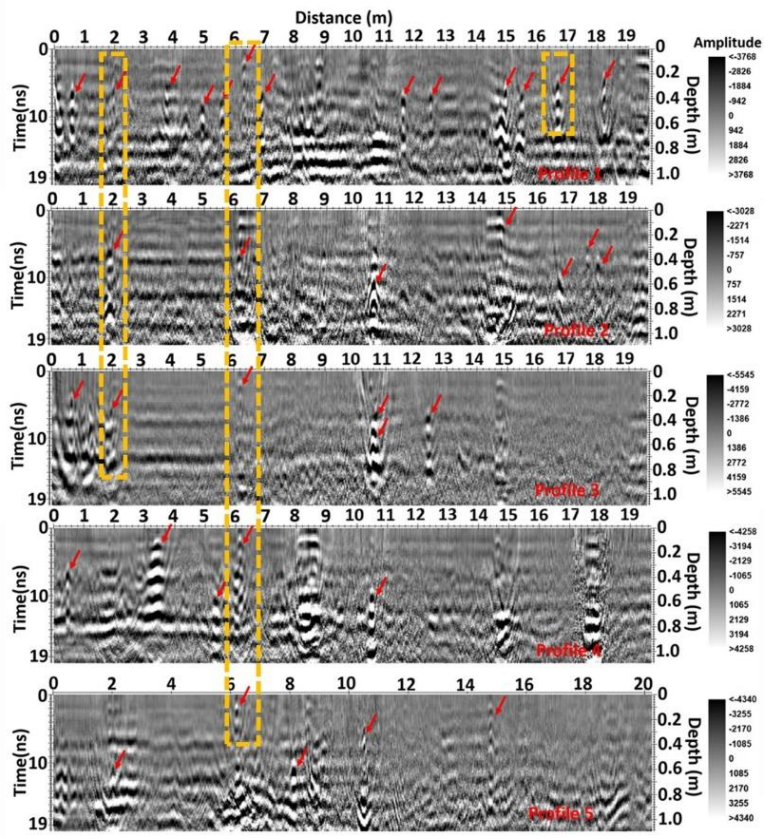

Figure 11. Diffraction 2D-velocity applied radargrams to the same profiles.

This type of migration was implemented to assess how the Kirchhoff 2D-velocity migration type results with the same speed fields on the GPR data obtained in Figure10 (Figure 12).

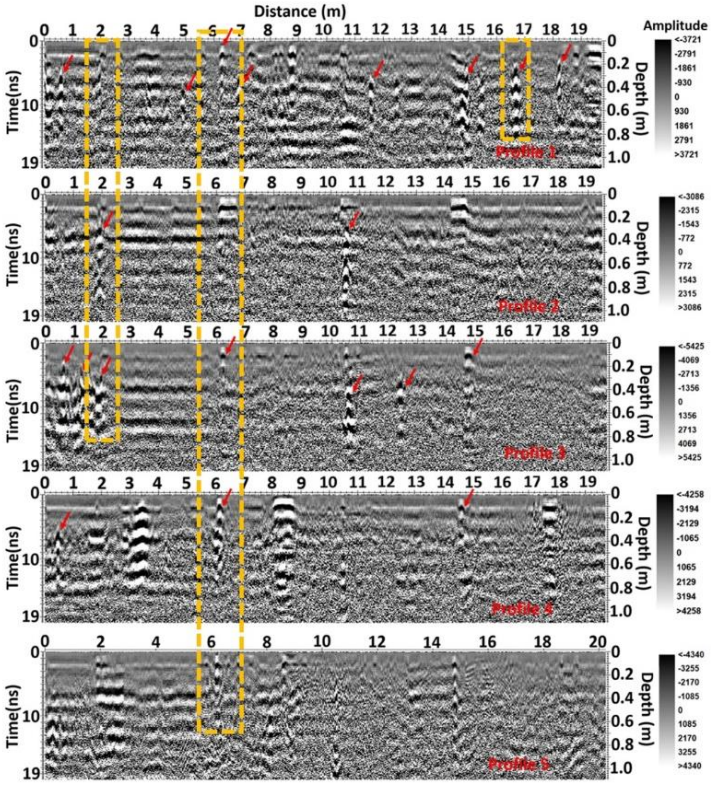

Figure 12. Kirchhoff 2D-velocity applied radargrams to the same profiles.

When we compare the results of these migrations applied in Figure 11 and 12, both migrations result in the correct positions of deterioration. However, in terms of resolution, the Diffraction 2D-velocity migration type yielded more accurate results than the Kirchhoff 2D-velocity migrations. During Kirchhoff 2D-velocity migration, the resolution decreased and remained weaker.

To examine the lateral and vertical changes of strong reflections in GPR sections obtained from the Zigana tunnel with fracture-crack, gap, and moisture content, amplitude slice maps were obtained from these sections. These maps were composed of the radargrams of the 5 profiles which were obtained in parallel in the same direction (Figures 13,14).

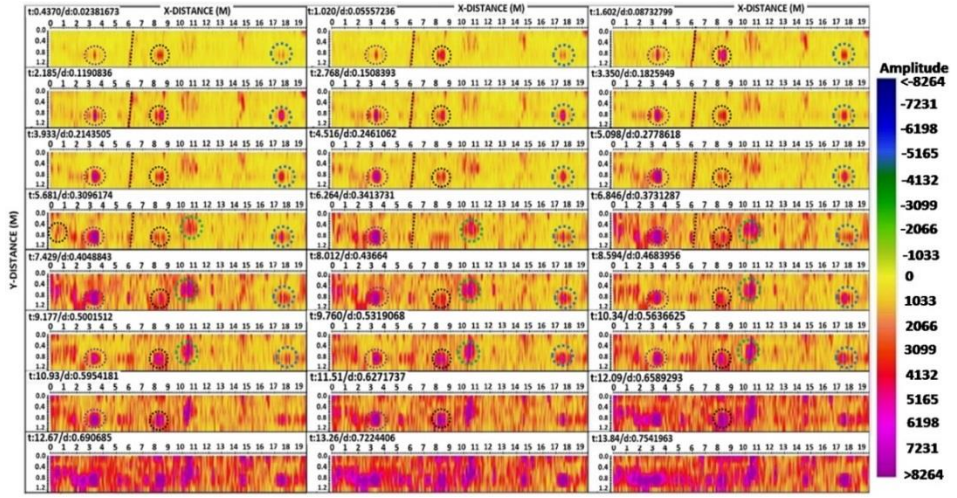

Figure 13. Zigana Tunnel: Amplitude slice maps for diffraction 2D-velocity migration step (2 -78 cm).

The amplitude slice maps obtained after applying the Diffraction 2D-velocity migration type to the radargrams of the 5 profiles were shown in Figure 13. When these maps were examined, a fracture of approximately 6m distance from the surface was observed to continue to a depth of 27 cm in the structure. Similarly, the fractures, water content and deterioration within the structure observed from the surface, were defined by dashed lines.

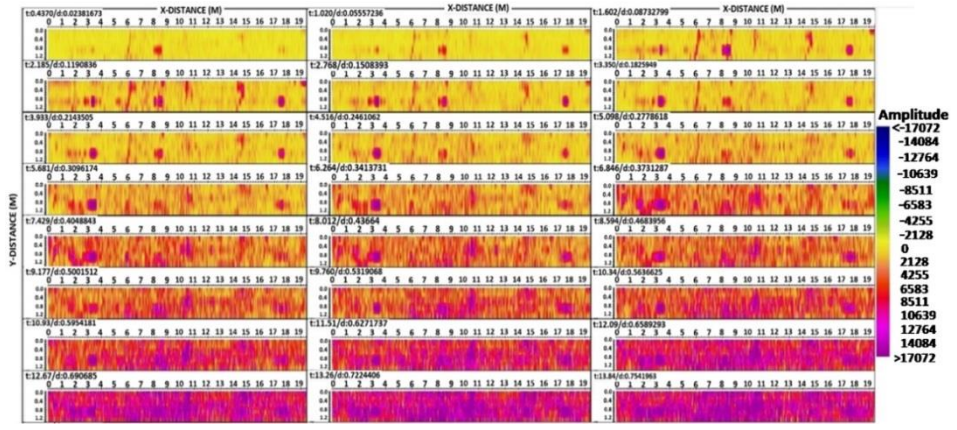

Figure 14. Zigana Tunnel: Amplitude slice maps for Kirchhoff 2D-velocity migration step (2-78 cm).

After applying the Kirchhoff 2D-velocity migration type to the same radargrams, amplitude slice maps were obtained in Figure 14. In these maps, as in Figure 13, the locations of the fractures are observed in the same positions. However, compared to the maps obtained in Figure 13, the Kirchhoff 2D-velocity migration type was not very successful in carrying distortions to the correct positions after a depth of 37 cm.

7. CONCLUSIONS

Within the scope of this study, radargrams were obtained for the monitoring of the depth-dependent variation of sections with fracture-cracks, gaps and moisture content in the first study, the Zigana tunnel wall of 43 years. In these radargrams, fracture-cracked parts in the structure, places with moisture content and deterioration which cannot be observed from the surface but thought to be within the structure were determined.

In the applications on concrete structures, some analysis techniques can be applied to the data collected by a high frequency antenna (500 MHz) in addition to data collection with antennas of the GHz level and the resolution can be increased. For this situation, the artificial radargram was formed based on the Finite Difference Time Domain method by modeling the Torul Tunnel wall which is known as the newly constructed structure. Diffraction 2D-velocity and Kirchhoff 2D-velocity migrations were applied to bring their correct positions to the scattered reflections at this radargram and the radargrams obtained from the Zigana tunnel wall. From the results of this migration, the Diffraction 2D-velocity type was observed to have more successful results in terms of better focusing and resolution of the reflectors.

Depending on the results of both migrations to the data obtained from the Zigana tunnel wall, amplitude slice maps were created to monitor the changes in the lateral and vertical directions of the strongest reflections. On these maps, the deteriorations as fracture-crack and moisture content in the structure was not fully determined after 37 cm depth in resolution Kirchhoff 2D-velocity migration type. In the analysis of the GPR images obtained in the visualization of the concrete wall interior structure, in the light of the results of these migrations generated depending on the velocity field, it is recommended to apply Diffraction 2D-velocity migration of the data obtained with the high frequency antenna (500 MHz).

Since the Zigana tunnel is built with the technology used in ancient times, the water leaks from the faults between the ore dacites, the environment where the building passes, and passes into the tunnel. These leaky waters damage the concrete coating and the structure over time due to the freezing and thawing events during the seasonal transitions. Given the history of the tunnel over a long period of time, it is estimated that concrete has been severely decomposed and dissolved over time. When these problems are generally evaluated, it is recommended to renew the tunnel concrete structure or to improve the concrete coating. Depending on these improvements, the factors that endanger the traffic safety and the stalactites of the water leaking through the tunnel structure will be prevented.

Acknowledgments

I would like to thank Rasim Taylan KARA for the contributions in the paper.

REFERENCES

[1] Pajewski L., Fontul S., and Solla M. (2019) Ground-penetrating radar for the evaluation and monitoring of transport infrastructures. Chapter 10, Innovation in Near-Surface Geophysics, Elsevier.

[2] Lehmann F. (2015) Practical application of non-destructive test methods at a single-shell tunnel lining, in: Proc. of the 7th fib PhD Symposium in Stuttgart, Germany Sept. 11-13.

[3] Salvi R., Ramdasi A., Kolekar Y., and Bhandarkar L.V. (2019) Use of Ground-Penetrating Radar (GPR) as an Effective Tool in Assessing Pavements—A Review. Geotechnics for Transportation Infrastructure pp 85-95.

[4] Moropoulou A., Lampropoulos K. C., Sotiropoulos P., and Papageorgiou C. (2019) The Plaka Bridge in Epirus: Ground Penetrating Radar Prospection of Surviving Parts of the Collapsed Bridge, to Provide Structural Information for Its Reconstruction, Nondestructive Evaluation and Monitoring Technologies, Documentation, Diagnosis and Preservation of Cultural Heritage pp 91-106.

[5] Sarı M., and Öztürk S. (2018) Detection of the complex ground problems by ground penetrating radar: Examples from Gümüşhane University, Sigma J Eng & Nat Sci. 36 (4), 1295-1308.

[6] Cao Y., Liu Q., and Tao L. (2019) Application of Ground Penetrating Radar for Detecting Grouting Quality in Highway Tunnel. 2019 IEEE 8th Joint International Information Technology and Artificial Intelligence Conference (ITAIC).

[7] Rathod H., Debeck S., Gupta R., and Chow B. (2019) Applicability of GPR and a rebar detector to obtain rebar information of existing concrete structures. Case Studies in Construction Materials, 11, e00240. doi:10.1016/j.cscm.2019.e00240.

[8] Lin C., Wang X., Li Y., Zhang F., Xu Z., and Du Y. (2020) Forward Modelling and GPR Imaging in Leakage Detection and Grouting Evaluation in Tunnel Lining. KSCE Journal of Civil Engineering (2020) 24(1):278-294 DOI 10.1007/s12205-020-1530-z.

[9] YuH Z., Ouyang Y.F., and Chen H. (2012) Application of Ground Penetrating Radar to Inspect the Metro Tunnel, in: Proc. of the 14th International Conference on Ground Penetrating Radar (GPR), June 4-8, Shanghai, China.

[10] Tillard, S., and Dubois, J.C., (1995) Analysis of GPR data: wave propagation velocity determination, J. Appl. Geophysics. 77–91.

[11] NPRA Norwegian Public Roads Administration. (2012) Report No. 127. Major Research and Development Project: Modern Road Tunnels 2008-201, NPRA, Oslo (Norwegian)

[12] Selahattin P. (1977) Alucra (Giresun) güneydoğu yöresinin petrol olanakları bakımından incelenmesi, Doçentlik Tezi, KTÜ, Yayın No:87, Trabzon, (yayımlanmamış).

[13] Güven, İ.H., 1993. Doğu Pontidlerin Jeolojisi ve 1/250.000 Ölçekli Kompilasyonu, MTA Yayınları, Ankara.

[14] Rasol M. A., Pérez-Gracia V., Fernandes F. M., Pais J. C., Santos-Assunçao S., Santos C., and Sossa V. (2020) GPR laboratory tests and numerical models to characterize cracks in cement concrete specimens, exemplifying damage in rigid pavement.

[15] Alsharahi G., and Driouach A. (2015) Simulation of Ground Penetrating Radar Imaging Under Subsurface.

[16] Conyers, L. B., and Goodman, D., (1997) Ground-penetrating radar: An Introduction for Archaeologists. California: Altamira Press.